



Beneficiation and Characterisation of Kaolin Clay from Clay Deposit in Kutigi, Niger State, Nigeria

Ogundipe F.O^{1a}., Saidu M^{2b}., Abdulkareem, A.S.^{3c}. & Busari, A.O^{2d}.

¹Federal Ministry of Water Resources, Abuja, Nigeria

²Department of Civil Engineering, Federal University of Technology, Minna, Nigeria

³Department of Chemical Engineering, Federal University of Technology, Minna, Nigeria

^aogundipefelix@yahoo.com; ^bm.saidu@futminna.edu.ng; ^ckasaka2003@futminna.edu.ng;

^dbusari.a@futminna.edu.ng

Corresponding author: ogundipefelix@yahoo.com

Abstract

Kaolin is widespread across Niger State in Nigeria, relatively free of charge, non-toxic and environmentally friendly. In this study, kaolin clay from Kutigi, Niger State, Nigeria was beneficiated and characterised for their crystal structure and morphology using X-Ray Diffractometer (XRD), Dispersive X – Ray Fluorescence (XRF) Machine, High Resolution Transmission Electron Microscope (HRTEM) and Brunauer – Emmett – Teller (BET) Nitrogen Absorption Analyser. The average crystallite size of the raw kaolin and Beneficiated Kaolin Clay (BKC) was calculated to be 40.258nm and 28.114nm respectively. The XRD analysis showed that the BKC had four (4) different phases of kaolinite: $Al(Si_2O_5)(OH)_4$, kaolinite 1Md – $AlSi_2O_5(OH)_4$, quartz – SiO_2 and muscovite – $KAl_2(Si_3Al)O_{10}(OH)_2$. XRF analysis showed a SiO_2/Al_2O_3 ratio of 1.54 and 1.35 in raw and BKC respectively. The Selected Area Electron Diffraction (SAED) pattern showed that the raw clay and BKC were polycrystalline in nature with each bright spots reflecting individual peaks. The Bet analyses showed that the adsorption-desorption isotherms for the BKC possessed pore size of mesopore widths between 13.8994 nm, surface area of $14.5126 m^2 g^{-1}$, pore volume of $0.003740 cm^3/g$ and adsorption average diameter of 1.0309 nm. This research work showed that kaolin clay from Kutigi is poly-crystallinity in nature and could be used as adsorbent for wastewater treatment.

Keywords: Beneficiation, Kaolin, Clay, Kutigi, Nigeria.

Introduction

Human society has been using clays and clay minerals since the stone age, primarily since clay minerals are common at the earth's surface and are widely utilized for agriculture (soils), ceramics and building materials with a very long history (Auta and Hameed, 2013; Murray, 2000; Saikia *et al*, 2003; Chun *et al*, 2013), Clay is used by engineering geologists and sedimentologists to describe geological materials of less than 4 μm in size, by soil scientists to denote the soil fraction containing particles of less than 2 μm size, and colloidal scientists of less than 1 μm (Chun *et al*, 2013). Clay materials are cheaper than activated carbons and their sheet-like structures also provide high specific surface area (Dhaval & Painter, 2017). The inherent features of clay minerals that make them attractive for use in a wide variety of applications include very large surface area that arises from the layered structure, along with its swell ability and the potential for delamination; small size of the particles in the range of micro- to nanoscale; and naturally charged particles leading to relatively strong electrostatic interactions (Chun *et al*, 2013). Pure kaolinite is white in colour and its chemical composition is 46.54% SiO_2 , 39.50% Al_2O_3 and 13.96% H_2O and presence of impurities, particularly iron and titanium bearing materials, imparts colour to kaolin (Saikia *et al*, 2003). The mined kaolin is usually associated with various impurities like quartz, anatase, rutile, pyrite, siderite and feldspar depending on the origin and depositional environment. Clay materials can be modified using a variety of chemical/physical treatments to achieve the desired surface properties for best immobilization of contaminants (Aroke and Onatola, 2016). Physical and chemical behaviours of clay minerals have been studied by numerous researchers due to their adsorbing and catalytic properties (Sachin *et al*, 2013). The three main groups of clay minerals are kaolinite, montmorillonite or smectite and illite. Kaolin is another aluminosilicate mineral which is found among different type of clays (Kuranga *et al* 2018; Karl *et al*, 1996; Yahaya *et al*, 2017). Kaolin is widespread across Niger State, relatively free of charge, non-toxic and environmentally friendly. Niger State produced a total of 51,149.80 tons of solid minerals in 2016 (RMRDC, 2012).

Materials and Methods

The kaolin clay sample was collected from a clay deposit in Kutigi in 20 kg capacity leather bag and transported to the National Water Quality Reference Laboratory Minna for further processing and



analyses. Kutigi Town is located at longitude 9° 12' 0" N and latitude 5° 36' 0" E. Removal of leaves and dead insects was done, and the kaolin clay oven dried at 105°C for 6 hours. The oven dried kaolin clay was crushed with a mortar and pestle, grinded to particle that could pass through a 250 µm mesh sieve to obtain very fine particles. The oven dried raw kaolin clay was processed by sedimentation technique to produce clay fractions of < 2 µm hydrodynamic diameter and removal of excess non-clay impurities. The kaolin clays were allowed to swell in distilled water for 22hrs 57mins to allow for proper intercalation of the clay structure by water molecules (Bachiri *et al*, 2014). The sedimentation of the slurries was monitored and done according to the Stoke's Law with the following formula:

$$u_s = \frac{g(\rho_p - \rho_w)d_p^2}{18\mu} \quad (1)$$

Where ρ_p = particle density, kg/m³ (Kaolin clay particle = 1600kg/m³); μ = liquid viscosity, kg/m.s (distilled water = 8.90×10^{-4} Pa.s); ρ_w = density of water, kg/m³ (997kg/m³); u_s = particle settling velocity, m/s; d_p = diameter of particle, m; g = acceleration due to gravity, m/s² (9.81m/s²); t = Settling Time; R = particle size (radius) of clay, assumed to be spherical (1µm = 1×10^{-6} m); h = Settling Height of Fluid.

The beneficiated kaolin clay was activated with 0.5M HCl, washed with 10% Hydrogen Peroxide (H₂O₂) to oxide organic matter (Bachiri et al, 2014) and distilled water until the pH 7 was obtained. The Mass of the activated BKC obtained was measured and the value substituted in the following equation to obtain the percentage yield of the kaolin clay.

$$Y = \frac{\text{Mass of Purified Kaolin Clay Produced}}{\text{Mass of Raw Kaolin Clay}} \times 100\% \quad (2)$$

The identification of phases and the crystallite sizes of the raw kaolin clay and BKC were determined using the Emma 0141 X-Ray Machine by GCB scientific Equipment. The phase identifications were done by comparison with available d-spacing information and peaks from International Centre for Diffraction Data (ICDD) and Powder Diffraction File (PDF). The interplanar spacing for diffraction angle of each peak (d-spacing) was calculated using Braggs law in the following equation. $n\lambda = 2d \sin \theta$; Where λ = wavelength of X-Ray = 1.5406 Å; d = d-spacing in Å, θ = Diffraction angle in radians. The unit cell parameters were calculated and indexed as $h k l$. Full Width at Half Maximum (FWHM) of the selected peak was determined using student version of OriginPro 2021b (trial) data and analysis software from OriginLab Corporation, Northampton, USA. The average crystallite size of the clay was calculated from the analysis of the peaks in the X-Ray diffractogram using the following Scherer Equation.

$$D = \frac{K\lambda}{\beta \cos \theta} \quad (3)$$

Where; λ = Wavelength of X-Ray, CuKa = 1.5406 Angstrom (Å), K =Scherer Constant (0.94 for spherical crystallites with cubic symmetry), β = Full Width at Half Maximum (FWHM) for the peaks in radians, θ = Bragg's diffraction angle in degrees

TECNAI G2 F20 twin model High Resolution Transmission Electron Microscope (HRTEM) was used for the analysis of particle size and distribution pattern of the raw and BKC. The surface area and pore volume of the BKC was determined using the TriStar II 3020 BET Nitrogen adsorption technique. The chemical analysis of the generated BKC was done using Dispersive X – Ray Fluorescence (XRF) machine (EDXRF-3600B) by Oxford instrument. Loss on Ignition (LOI) test was conducted on the raw and purified kaolin clay to determine the mass of the volatile matters present in each sample tested.

Results And Discussion

The yield of kaolin clay fractions of less than 2 µm from the raw kaolin clay is presented in Table 1. The yield increased with increase in the percentage slurry from 2.5 %, w/w to 5 %, w/w and remained constant at 7.5 %, w/w and 10 %, w/w. The lower yield experienced at 7.5 and 10 %, w/w slurry could be attributed to the repulsion forces between the negatively charged clay particles which were free in the suspension and hence prevented particles from settling at the experimental calculated time of 22hrs 57mins (Table 2) for particles of less than 2 µm.



Table 67: Yield of Beneficiated Kaolin Clay

Kaolin Clay Slurry	Dried Mass of Raw Sample (g)	Dried Mass of Beneficiated Kaolin Clay (g)	Yield (%)	Settling Height (cm)
2.5 %, w/w	100	7.60	7.60	8.10
5.0 %, w/w	200	18.3	9.15	12.0
7.5 %, w/w	300	27.4	9.13	9.20
10 %, w/w	400	36.5	9.13	9.20

The kaolin clay slurries during the sedimentation technique were allowed to settle according to Stoke’s Law and the settling time result along with the other design parameters for purification of the kaolin clay are presented in Table 2. The soil particles are denser than water, they tend to sink, settling at a velocity that is proportional to their size. The speed at which the kaolin particles settled during the purification process was 1.477×10^{-6} m/s. The settling time was calculated to be 22hrs 57mins.

Table 68: Kaolin Clay Sedimentation Design Parameters

Parameters	Results	Remarks
Liquid Viscosity, kg/m.s	8.90×10^{-4} kg/m.s	Viscosity of Distilled Water
Kaolin Clay Particle Density, kg/m ³	1600kg/m ³	Particle Density
Density of Water, kg/m ³	997kg/m ³	Density of Water
Acceleration due to Gravity, m/s ²	9.81m/s ²	Gravitational Force
particle size (radius) of kaolin clay, m	$1\mu\text{m} = 1 \times 10^{-6}$ m	assumed to be spherical
Settling Height, m	0.12m	Measurement of the Supernatant
Kaolin clay Settling Velocity, m/s	1.477×10^{-6} m/s	Calculated using Stoke’s Law
Kaolin Clay Settling Time, hrs	22hrs 57mins	Calculated using Stoke’s Law

The physicochemical properties of the raw and beneficiated kaolin were presented in Table 3. The pH values of the raw and beneficiated clay were 5.60 and 7.02 respectively. The pH value of the beneficiated clay is slight neutral and will promote pollutants precipitation and adsorption. The organic matter in the raw kaolin clay could be attributed to the presence of dead animals and insects. The cation exchange capacity (CEC) of the raw kaolin clay and beneficiated clay were 8.65 and 12.5 meq/100g. The CEC characteristic would make the beneficiated kaolin clay play an important role in the adsorption of metal ions. The Electrical Conductivity (EC) of the beneficiated clay was higher than that of the raw kaolin clay. The higher EC in the beneficiated kaolin showed that it contained dissolved salts that could allow for the removal of phosphate, nitrate and some toxic metal ions in the domestic wastewater.

Table 69: Selected Physicochemical Properties of Raw and Beneficiated Kaolin

Parameters	Raw Kaolin Clay	Beneficiated Clay
Colour	Off White	White
Particle Shape	Spherical	Spherical
Texture	Coarse	Fine
pH	5.60	7.02
Organic Carbon, %	0.045	0.00
Cation Exchange Capacity (CEC), meq/100g	8.65	12.5
Electrical Conductivity, $\mu\text{S/cm}$	245	297
Density, g/cm ³	2.70	2.60
Viscosity (cP)	6.69	6.89

XRD diffractograms of raw kaolin clay and BKC displayed the existence of four crystalline phases of kaolinite – $\text{Al}(\text{Si}_2\text{O}_5)(\text{OH})_4$, kaolinite 1Md – $\text{AlSi}_2\text{O}_5(\text{OH})_4$, quartz – SiO_2 and muscovite – $\text{KAl}_2(\text{Si}_3\text{Al})\text{O}_{10}(\text{OH})_2$. These four identified phases were chemically identical, but their atoms were arranged differently except that of muscovite that contained potassium (Tables 4 and 6). The dominated impurity compound in the raw kaolin clay and BKC was quartz with 66.41 % and 46.85% respectively. Multiple peaks were detected for each phase between 5.077° to 85.049° . The best peaks produced at the Full Width at Half Maximum (FWHM) of the intense peak for raw kaolin clay and BKC ranged from 0.1588 – 0.40475 radians and 0.1825 – 0.5118 radians respectively. The broad peaks formation of the XRD

pattern for both raw kaolin clay and PKC showed that they were both polycrystalline in nature. The XRD pattern showing various peaks produced in the characterisation of raw kaolin clay and BKC is presented in Figure 1. Interplanar spacing between the parallel planes of atoms in raw kaolin clay and BKC were 3.4994 nm and 3.532nm at Scherrer’s constant of 0.94 and wavelength (λ) of 1.5406 Å. The average crystallite size for the raw kaolin clay and BKC were calculated to be 40.258nm and 28.114nm as shown in Tables 5 and 7.

Table 70: XRD Phase Identification of Raw Kaolin Clay

Phases	Formula	Percentage (%)
Kaolinite	$Al(Si_2O_5)(OH)_4$	14.10
Kaolinite	$AlSi_2O_5(OH)_4$	15.04
1Md		
Quartz	SiO_2	66.41
Muscovite	$KAl_2(Si_3Al)O_{10}(OH)_2$	4.45

The average crystallize size (28.114nm) of beneficiated kaolin clay were less than that of raw kaolin clay (40.258nm). The lower the crystallize size the higher the surface area. This implied that the beneficiated clay would be more potent in the contaminant’s removal from domestic wastewater than the raw kaolin clay. The crystallite size is an important parameter as the sizes of the crystals determine whether the material is soft (small crystallites) or brittle (large crystallites), as well as thermal and diffusion behaviour of semicrystalline polymers (Sanjeeva, 2013).

Table 71: Interplanar Spacing and Crystallite Size of Raw Kaolin Clay

Diffraction Angle, 2θ	d- spacing, (nm)	FWHM of the Intense Peak, β , (radians)	Crystallite Size, D, (nm)
12.2860	7.2203	0.25190	33.129
24.8213	3.5950	0.32526	26.120
26.5769	3.3613	0.15880	53.688
50.0630	1.8258	0.14218	64.408
62.2406	1.4945	0.40475	23.946
Average	3.4994		40.258

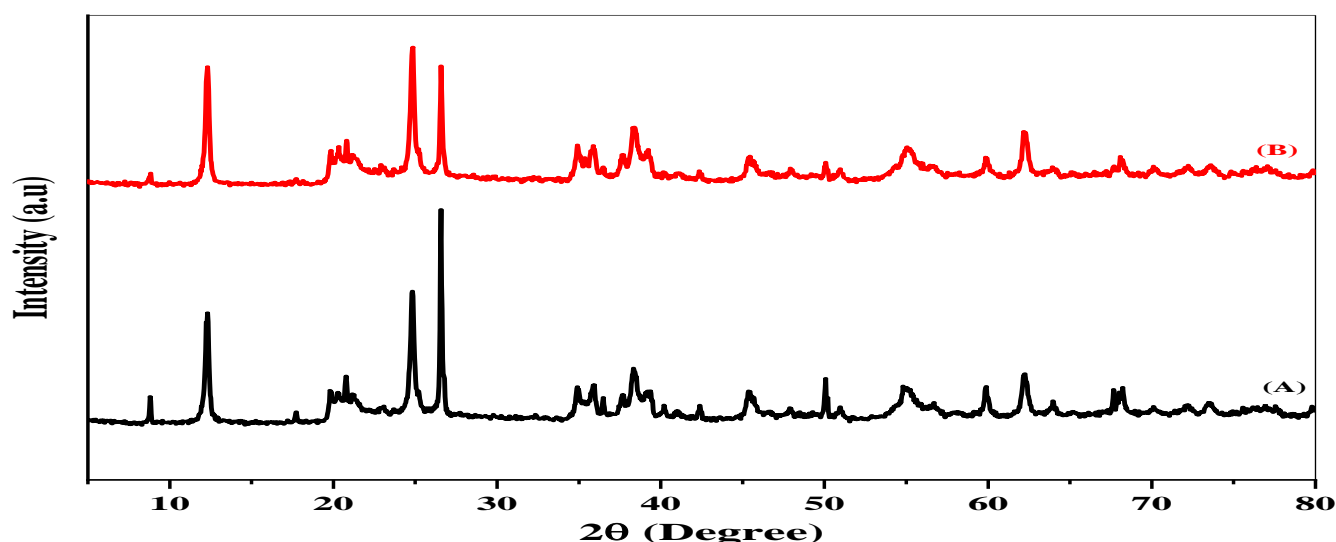


Figure 11: XRD patterns of (A) Raw kaolin and (B) beneficiated kaolin

Table 72: XRD Phase Identification of Beneficiated Clay

Phases	Formula	Percentage
Kaolinite	Al(Si ₂ O ₅)(OH) ₄	28.52
Kaolinite 1Md	AlSi ₂ O ₅ (OH) ₄	19.01
Quartz	SiO ₂	46.85
Muscovite	Kal ₂ (Si ₃ Al)O ₁₀ (OH) ₂	5.62

Table 73: Interplanar Spacing and Crystallite Size of Beneficiated Clay

Diffraction Angle, 2θ	d- spacing, (nm)	FWHM of the Intense Peak, β, (radians)	Crystallite Size, D, (nm)
12.2966	7.2142	0.3106	26.869
24.8279	3.5940	0.3225	26.348
26.5858	3.3602	0.1825	46.714
45.5049	1.9975	0.5118	17.580
62.2534	1.4942	0.4203	23.060
Average	3.532		28.114

Table 8 shows the results of chemical analysis of the raw and beneficiated kaolin clay. The raw kaolin clay contained alumina (34.18%) and silica (52.64%) in large quantities. The beneficiated kaolin clay contained alumina of 35.95 % and silica of 48.55% respectively. The proximity of silicate and alumina compositions obtained in the raw and beneficiated kaolin showed that raw kaolin has silicate more than beneficiated kaolin clay and the beneficiated kaolin clay contained alumina more than the raw kaolin. The loss of silicate and the gain of alumina in the beneficiated kaolin clay could be attributed to the purification and treatment method employed for the beneficiation of the kaolin clay. The SiO₂/Al₂O₃ ratio of kaolin clay which is a function of the mineral phase present was found to be 1.54 and 1.35 in raw and beneficiated kaolin clay respectively. Clay minerals are classified by the ratio of their silica and alumina sheets. The SiO₂/Al₂O₃ ratio of beneficiated clay (1.35) as gotten in this study showed a purer kaolinite than the raw clay. Loss on ignition (LOI). LOI for raw and beneficiated kaolin were 8.90% and 11.62% respectively. The high LOI for beneficiated clay is attributed to the dehydroxylation reaction in the kaolin mineral. High LOI for beneficiated clay was also an indication of potential normal porosity in the intended kaolin clay filter adsorbent for treatment of domestic wastewater.

Table 74: Mineralogical composition (XRF) of Raw and Beneficiated Clay

Compound	Raw Kaolin Clay (%)	Beneficiated Kaolin Clay
Fe ₂ O ₃ %	1.23	1.24
MnO %	0.00	0.00
Cr ₂ O ₃ %	0.02	0.02
V ₂ O ₅ %	0.00	0.00
TiO ₂ %	1.69	1.75
CaO %	0.33	0.02
K ₂ O %	0.61	0.63
P ₂ O ₅ %	0.07	0.05
SiO ₂ %	52.64	48.55
Al ₂ O ₃ %	34.18	35.95
MgO %	0.23	0.03
Na ₂ O %	0.11	0.14
LOI %	8.90	11.62
Total	100	100
SiO ₂ /Al ₂ O ₃ Ratio	1.54	1.35

The crystal patterns of the raw kaolin clay are presented in Plate I (a – e). HRTEM of raw kaolin clay showed kaolinite particles of varying sizes arranged in face-to-face patterns. The crystallinity of the raw kaolin clay structure was examined using Selected Area Electron Diffraction (SAED) pattern in Plate I (f). The SAED pattern showed concentric circles of polycrystallinity. The bright spots and rings of the SAED pattern suggested that the raw kaolin clay is polycrystalline in nature and each ring depicted diffraction pattern of crystals of similar size with each bright spots reflecting individual peaks. SAED resolution pattern obtained were consistent with the results of XRD and XRF characterisation in this study. EDX analysis of the raw kaolin clay showed the presence of Oxygen, Aluminium and Silicon

with minor amounts of Potassium, Titanium and Iron. The % atomic weight and % weight sigma of elements identified by the EDX analysis for raw and beneficiated kaolin clay is presented in Table 9. HRTEM images in Plate II (a – e) showed the structure of the beneficiated kaolin clay. HRTEM of beneficiated clay showed kaolinite particles of varying sizes arranged in face-to-face patterns. The crystal structure in Plate II (f) showed bright rings of the SAED patterns that are polycrystalline in nature. Each ring depicted the diffraction pattern of purified kaolin clay particles.

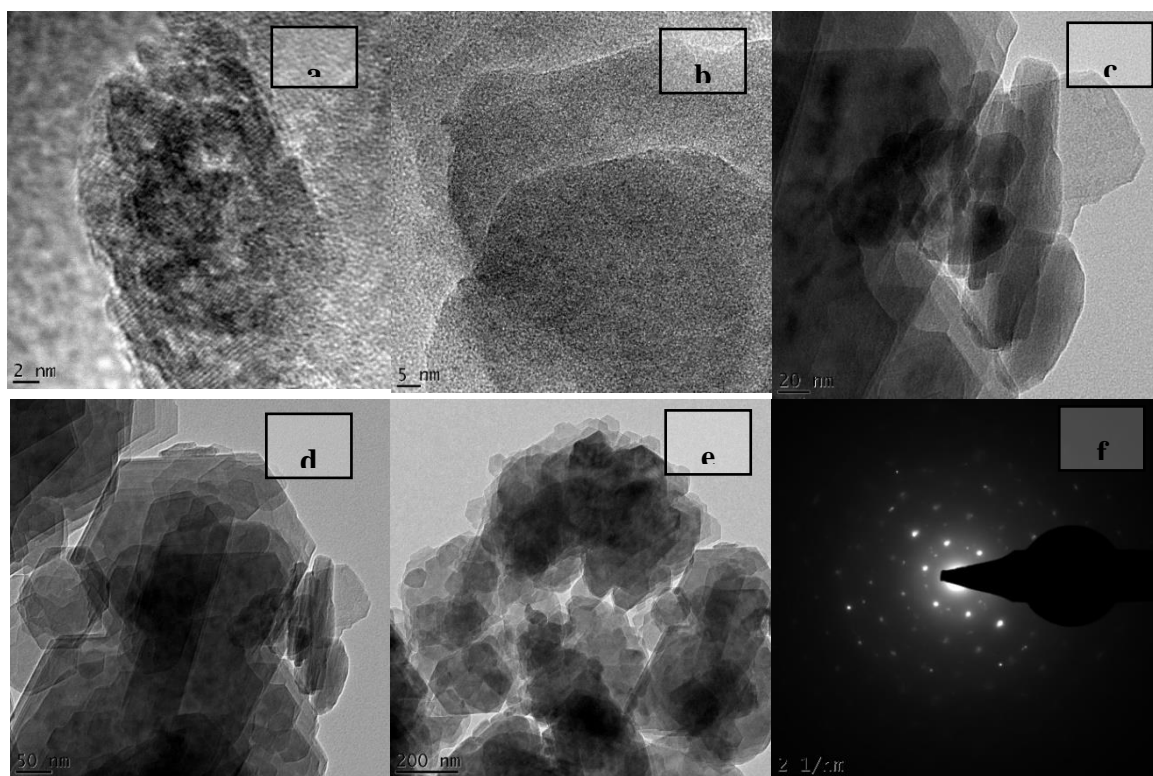


Figure 12: Plates showing HRTEM (a – e) and SAED (f) Images of Raw Kaolin Clay

Table 75: EDX Analysis of Raw Clay

Element	%weight	%weight Sigma
O	47.6	0.24
Al	22.7	0.15
Si	26.7	0.17
K	0.42	0.05
Ti	1.19	0.07
Fe	1.43	0.09
Total:	100	0.77

The EDX point micrograph showed the presence of Oxygen, Aluminium and Silicon with minor amounts of Potassium, Titanium and Iron. The % atomic weight and % weight sigma of elements identified by the EDX analysis for beneficiated kaolin clay is presented in Table 10. Although, the raw and the beneficiated kaolin clay exhibited similar morphologies based on EDX results, their elemental constituent differed. As it could be seen, the major difference may be attributed to the percentage reduction of iron, oxygen and aluminium and increase in presence of potassium, silicon and titanium in the beneficiated clay. These results suggested that there would be a possibility of cation exchange between the beneficiated kaolin clay and metal ions during treatments. This could enhance high adsorption capacity and improve removal efficiency of pollutants by the beneficiated kaolin clay. These results are consistent with the XRD and XRF results as earlier discussed.

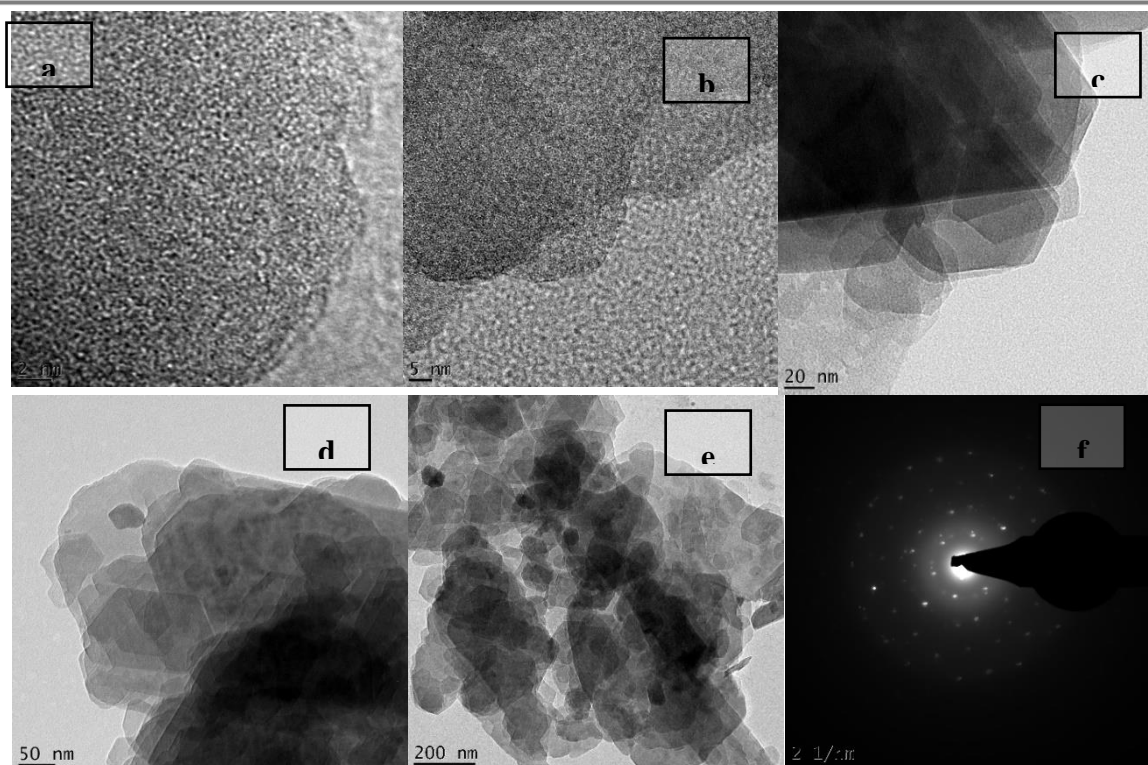
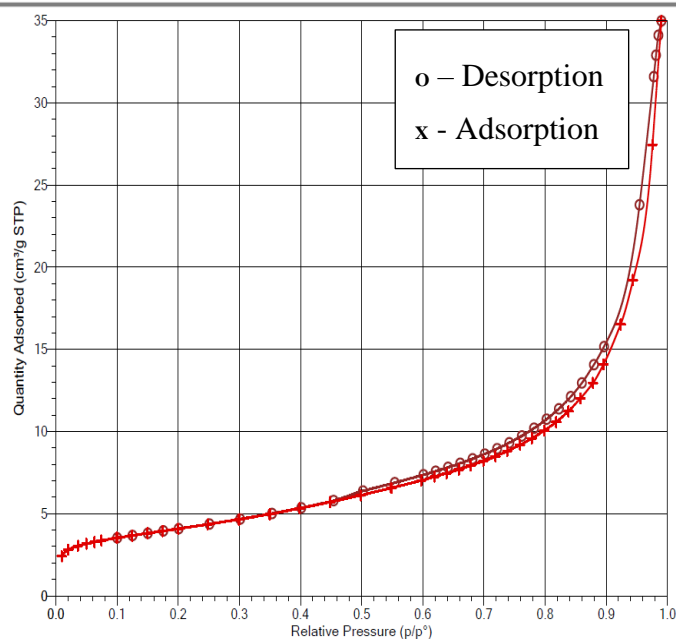


Figure 13: Plate showing HRTEM (a – e) and SAED (f) Images of Beneficiated Kaolin Clay

Table 76: EDX Analysis of Beneficiated Kaolin Clay

Element	% Weight	% Weight Sigma
O	46.92	0.26
Al	21.42	0.16
Si	28.34	0.19
K	0.53	0.05
Ti	1.48	0.08
Fe	1.30	0.10
Total:	100	0.84

Nitrogen (N_2) adsorption-desorption isotherm showed that the beneficiated kaolin clay belongs to type IV isotherm with a hysteresis loop (Figure 2), which resulted from capillary condensation in the mesopores (diameter, $2 < d < 50$ nm) at the relative pressure range of 0.45 – 0.9, P/P_0 . When the relative pressure was 0.4 – 0.9 P/P_0 , the desorption branch was obviously higher than the adsorption branch, along with the appearance of capillary condensation, which resulted in the hysteresis loop. At the relative pressure of 0.4 – 0.9 P/P_0 , the adsorption branch and desorption branch suddenly rose and coincided at the end (Figure 2). Therefore, the occurrences of hysteresis loops indicated that the beneficiated kaolin clay had a lot of mesopores. The quasi-overlapping adsorption-desorption curves indicated that the N_2 adsorption-desorption isotherm curve of the beneficiated kaolin clay can be classified as Type IV, indicating a purely mesoporous material with small pore size. Furthermore, the IUPAC classified Hysteresis Loops into four types, each type representing a different pore shape (Xu *et al*, 2020). Accordingly, hysteresis loops of the beneficiated kaolin clay belong to type H3, demonstrating that wedge-shaped pores took the primary position in the beneficiated kaolin clay.



The adsorption-desorption isotherms for the beneficiated kaolin clay possessed pore sizes that fell in the BJH desorption average pore width of 13.0470nm (Table 13). The BET surface area of beneficiated kaolin clay was 14.5126 m²g⁻¹, the single point adsorption total pore volume was 0.003740 cm³/g, adsorption average diameter was 1.0309 nm and BJH adsorption average pore width was 13.8994nm. Strong adsorbents used for water treatment have large surface areas (Worch, 2012). The BET analysis results showed the beneficiated kaolin clay as promising materials that could be used as adsorbent for filter production

Figure 14: BET Analysis of Beneficiated Kaolin

Conclusion

The beneficiation of Kutigi kaolin clay produced a crystallite size of 28.114nm. XRF analysis reflected a SiO₂/Al₂O₃ ratio of Kutigi kaolin clay and BKC to be 1.54 and 1.35 respectively. The crystal structure and morphology of BKC showed that kaolinite particles of varying sizes were arranged in face-to-face patterns with the bright spots and rings of the SAED pattern suggested that the raw clay and BKC were polycrystalline in nature. BET surface area for the BKC was determined to be 14.5126 m²g⁻¹, pore volume was 0.003740 cm³/g and adsorption average diameter was 1.0309 nm. BJH adsorption average pore width was found to be 13.0470 nm.

Acknowledgement

OriginLab Corporation, Northampton, USA: Provision of Student version of OriginPro 2021b (trial) data and analysis software to calculate Full Width at Half Maximum (FWHM) of the selected peak. Federal Ministry of Water Resources Abuja, Nigeria: Free access to National Water Quality Reference Laboratory Minna. Nanotech Research Group, Federal University of Technology, Minna: Interfacing and liaising with the University of South Africa to characterize the kaolin clay and BKC samples.

References

- Aroke U. O. and Onatola-Morakinyo S. (2016). Comparative Sorption of Diatomic Oxyanions onto HDTMA-Br Modified Kaolinite Clay. *International Journal of Engineering and Science* Vol.6, Issue 7 (August 2016), PP -01-09 Issn (e): 2278-4721, Issn (p):2319-6483, www.researchinventy.com
- Auta M. and Hameed B.H. (2013). Acid modified local clay beads as effective low-cost adsorbent for dynamic adsorption of methylene blue. *Journal of Industrial and Engineering Chemistry*, 1153–1161, <http://dx.doi.org/10.1016/j.jiec.2012.12.012>
- Bachiri El .M., Akichouh El Miz .H., Salhi S. and Tahani A. (2014). Adsorptions desorption and kinetics studies of Methylene Blue Dye on Na-bentonite from Aqueous Solution. *IOSR Journal of Applied Chemistry (IOSR-JAC)* e-ISSN: 2278-5736. Volume 7, Issue 7 Ver. III. (July. 2014), PP 60-78 www.iosrjournals.org
- Chun Hui Zhou and John Keeling (2013). Fundamental and applied research on clay minerals: From climate and environment to nanotechnology. *Applied Clay Science* 74 (2013) 3–9. <http://dx.doi.org/10.1016/j.clay.2013.02.013>
- Dhaval Patel and Z.Z.Painter (2017). Batch and Column Study for Treatment of Sugar Industry Effluent by using low-cost Adsorbent. Vol-3 Issue-3 2017 *IJARIE-ISSN(O)-2395-4396*
- Karl Terzaghi, Ralph B. Peck and Gholamreza Mersi (1996). *Soil Mechanics in Engineering Practice*. Third edition published by John Wiley and Sons Inc., New York, USA



- Kuranga I.A, Alafara A.B, Halimah, Fb, Fausat A.M., mercy O.B. and Tripathy B.C. (2018). Production and Characterization of Water Treatment Coagulant from locally sourced Kaolin Clays. *J. Appl. Sci. Environ. Manage.* January, Vol. 22 (1) 103-109. DOI: <https://dx.doi.org/10.4314/jasem.v22i1.19>
- Murray Haydn H. (2000). Traditional and new applications for kaolin, smectite, and palygorskite: a general overview. *Applied Clay Science* 17 _2000. 207–221
- NBS. (2017). State Disaggregated Mining and Quarrying Data. *National Bureau of Statistics*, Nigeria.
- RMRDC. (2018). National Distribution of Raw Materials – Niger State
- Saikia N.J., Bharali D.J., Sengupta P., Bordoloi D., Goswamee R.L., Saikia P.C. and Borthakur P.C. (2003). Characterization, beneficiation and utilization of a kaolinite clay from Assam, India. *Applied Clay Science* 24 (2003) 93– 103. doi:10.1016/S0169-1317(03)00151-0
- Sachin Kumar, Achyut Kumar Panda and R. K. Singh (2013). Preparation and Characterization of Acids and Alkali Treated Kaolin Clay. *Bulletin of Chemical Reaction Engineering and Catalysis*, 8 (1), 2013, 61 – 69, <http://bcrec.undip.ac.id>
- Sanjeeva Murthy, N. (2013). Scattering techniques for structural analysis of biomaterials. *Characterization of Biomaterials*, 34–72. doi:10.1533/9780857093684.34 10.1533/9780857093684.34
- Worch E. (2012). *Adsorption Technology in Water Treatment Fundamentals, Processes, and Modeling*. Walter de Gruyter GmbH and Co. KG, Berlin. 345pp.
- Xu, L., Zhang, J., Ding, J., Liu, T., Shi, G., Li, X., ... Guo, R. (2020). *Pore Structure and Fractal Characteristics of Different Shale Lithofacies in the Dalong Formation in the Western Area of the Lower Yangtze Platform*. *Minerals*, 10(1), 72. doi:10.3390/min10010072 10.3390/min10010072, downloaded on 20 – 12 - 2022
- Yahaya Shehu, Suzi Salwah Jikan, Nur Azam Badarulzaman and Ajiya Dahiru Adamu (2017). Chemical Composition and Particle Size Analysis of Kaolin, *Path of Science*. Vol. 3, No 10 ISSN 2413-9009. DOI: 10.22178/pos.27-1